ELSEVIER

Thermochimica Acta 246 (1994) 129–140

thermochimica acta

Kinetic analysis of the hydration of $3CaO \cdot 3Al_2O_3 \cdot CaSO_4$ and the effect of adding $NaNO_3$

Shuguang Hu [a], Huixian Yang [a], Shaopong Liu [a], Dun Chen [b,1], David Dollimore [b,*]

[a] *Department of Materials Engineering, The Wuhan University of Technology, Hubei 430070, People's Republic of China*

[b] *Department of Chemistry, The University of Toledo, 2801 W. Bancroft Street, Toledo, OH 43606, USA*

Received 1 December 1993; accepted 6 April 1994

Abstract

$3CaO \cdot 3Al_2O_3 \cdot CaSO_4$ is the main component of the sulpho-aluminate early-strength cements. Its hydration properties decide the strength and long-term stability of the hydrated cement paste. In this article, such hydration properties and the effect of hydration temperature, as well as the addition of $NaNO_3$, on the hydration process are studied. Using the Calvet conducting C80 microcalorimeter, the rate of production of hydration products was determined quantitatively and the total hydration heats calculated. The kinetic parameters for the hydration process at different hydration temperatures and different hydration periods are also calculated. The change of kinetic parameters between those of pure $3CaO \cdot 3Al_2O_3 \cdot CaSO_4$ and those with added $NaNO_3$ are discussed, and are used to explain the anti-freezing properties of $NaNO_3$ on the hydration of cements.

Keywords: Calorimetry; Cement; DSC; Hydration; Kinetics; Microcalorimetry; XRD

1. Introduction

Sulpho-aluminate cements have certain unique characteristics and this has determined their use in various situations. This series of cements is classified as Type K

* Corresponding author.

[1] To whom enquires should be made concerning reprints.

SSDI 0040-6031(94)01833-3

in the United States but it may also be described as a shrinkage-compensation cement, an expansive cement or a self-stressing cement, etc. This particular series of cements is mainly composed of calcium sulpho-aluminate ($3CaO \cdot 3Al_2O_3 \cdot CaSO_4$) and β-dicalcium silicate (β-$2CaO \cdot SiO_2$). By adjusting the amount of added gypsum ($CaSO_4 \cdot H_2O$), various properties such as rapid hardening, early strength, shrinkage compensation, expansive and self-stressing can be obtained. The application of this series of cements is still being explored and studied [1,2].

In clinker form, sulpho-aluminate cements generally contain at least 60 wt% of $3CaO \cdot 3Al_2O_3 \cdot CaSO_4$. In the hydration process, this material reacts with gypsum to form ettringite ($3CaO \cdot Al_2O_3 \cdot 3CaSO_4 \cdot 31H_2O$) and alumina gel ($Al(OH)_3$). The reaction may be represented as

$$3CaO \cdot 3Al_2O_3 \cdot CaSO_4 + 2(CaSO_4 \cdot 2H_2O) + 34H_2O \rightarrow 3CaO \cdot Al_2O_3 \cdot 3CaSO_4 \cdot 31H_2O + 4Al(OH)_3 \quad (1)$$

From Eq. (1), when the mole ratio between $3CaO \cdot 3Al_2O_3 \cdot CaSO_4$ and $CaSO_4 \cdot 2H_2O$ is 1:2, all the $3CaO \cdot 3Al_2O_3 \cdot CaSO_4$ will be transformed into ettringite. If there is not enough gypsum, the hydration process will be

$$3CaO \cdot 3Al_2O_3 \cdot CaSO_4 + 18H_2O \rightarrow 3CaO \cdot Al_2O_3 \cdot CaSO_4 \cdot 12H_2O + 4Al(OH)_3 \quad (2)$$

It can be seen that the amount of gypsum decides the reaction path. These products are the main components of hardened sulpho-aluminate cement paste. They decide the strength and long-term stability of the cement paste.

$NaNO_3$ is one of the anti-freeze additives for concrete. It also acts as an anti-rust additive for steel-embedded constructions and as a plasticizer for cement paste. As an additive for winter construction of sulpho-aluminate early-strength cement, $NaNO_3$ shows very desirable properties such as the lowering of the liquid freezing point in concrete and the improvement of the hydration and hardening process in cement [3].

Although sulpho-aluminate cements have been used for several decades, research on the hydration process has mainly dealt with the mechanism of expansion [4–7]. No studies on the hydration kinetics have been reported. In this article, by taking advantage of the high sensitivity and accuracy of the Calvet conducting C80 microcalorimeter, the effects of hydration temperature and the addition of $NaNO_3$ on the hydration of $3CaO \cdot 3Al_2O_3 \cdot CaSO_4$ are analyzed. Hydration properties are also discussed. By quantitatively measuring the amount of products, kinetic parameters for the hydration process are calculated.

2. Experimental

2.1. Materials

Analytical grade chemicals, calcium carbonate ($CaCO_3$), aluminum oxide (Al_2O_3) and calcium sulfate ($CaSO_4 \cdot 2H_2O$), were used to obtain the appropriate

mixtures calculated from the formula $3CaCO_3 \cdot 3Al_2O_3 \cdot CaSO_4 \cdot 2H_2O$. All reagents were ground and passed through a sieve #180 ($<80\ \mu m$). The sample was mixed thoroughly and the appropriate amount of water was added to form a compact about 10 mm thick and 25 mm in diameter under pressure. After sintering the wet compact at a temperature of 1400°C for 4 h, it was cooled in air and ground immediately to pass sieve #180. After checking by X-ray diffractometry that it was synthesized successfully, the sample was stored in a desiccator.

The hydration process was interpreted according to Eq. (1) using the appropriate ratio of reactants. The weight of solid was about 250 mg and the water-to-solid ratio was 10. The percentage of $NaNO_3$ added was 2 wt% against $3CaO \cdot 3Al_2O_3 \cdot CaSO_4$. This is the percentage weight range which is utilized in industrial applications of this type but it is recognized that the effect noted is a function of the amount of accelerator added.

2.2. Apparatus

X-ray diffraction was performed on a D/max-III X-ray diffractometer. The testing power was 30 kV and the current was 40 mA. A Calvet conducting C80 microcalorimeter was used for the hydration process and as the differential scanning calorimeter (DSC), with α-Al_2O_3 as the reference material. Its heat sensitivity was 10 mW and the instantaneous energy sensitivity was 1 mJ. All the data were processed on a HP86B computer. The hydration temperatures used were 30, 45 and 60°C for pure $3CaO \cdot 3Al_2O_3 \cdot CaSO_4$ samples and 45°C for the sample with $NaNO_3$.

3. Results and discussion

The hydration data collected by the Calvet C80 microcalorimeter are discussed under four headings: hydration curves of the pure $3CaO \cdot 3Al_2O_3 \cdot CaSO_4$ samples at different temperatures, the effect of $NaNO_3$ on the hydration of $3CaO \cdot 3Al_2O_3 \cdot CaSO_4$ calculation of kinetic parameters for hydration at 45°C, and the effect of hydration temperature on the kinetic results for the pure $3CaO \cdot 3Al_2O_3 \cdot CaSO_4$ samples.

3.1. Hydration curves of the pure $3CaO \cdot 3Al_2O_3 \cdot CaSO_4$ samples at different temperatures

Fig. 1 shows the hydration curves of pure $3CaO \cdot 3Al_2O_3 \cdot CaSO_4$ at different temperatures. Based on the hydration curves, some hydration parameters are listed in Table 1. From Fig. 1 and Table 1, the following comments can be made about the behavior of the process at different temperatures. (1) At the beginning of the hydration, there is an initial reaction peak followed by a slow reaction period which is called the induction period. It is apparent from the experimental results that the induction period becomes shorter as the hydration temperature increases. (2) After

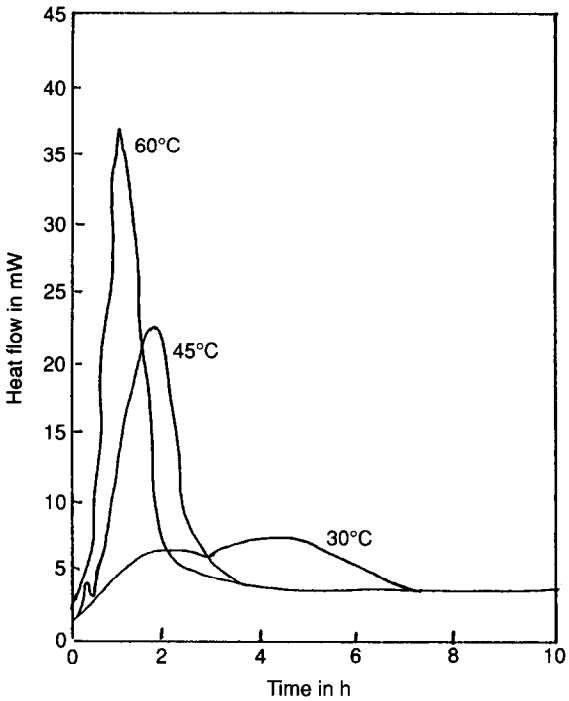

Fig. 1. Heat evolution curves for the hydration of $3CaO \cdot 3Al_2O_3 \cdot CaSO_4$.

Table 1
Hydration properties under different temperatures for $3CaO \cdot 3Al_2O_3 \cdot CaSO_4$

Temperature in °C	k_1 [a] in J g^{-1} h^{-1}	t_1 [b] in h	q_1 [c] in J g^{-1}
30	54	0.67	264.68
45	288	0.37	338.54
60	576	0.29	341.26

[a] The highest hydration rate. [b] The time when the induction period ends. [c] The accumulated hydration in 24 h.

the induction period, the reaction passes over into an acceleration period. In this period, the hydration rate increases as the hydration temperature increases and this is shown by the large hydration heat peak. The highest hydration rate (k_1 in Table 1) also follows the same trend. At the same time, the integrated hydration heat up to 24 h increases as the hydration temperature increases which means a higher degree of hydration is achieved.

From the discussion, the hydration process of $3CaO \cdot 3Al_2O_3 \cdot CaSO_4$ can be seen to be very similar to that of $3CaO \cdot SiO_2$ in Portland Cement. It can be divided into various stages: the initial period, the induction period, the acceleration period, the

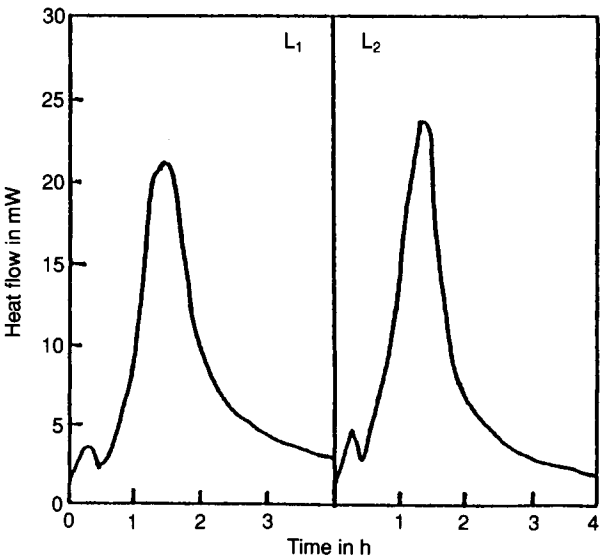

Fig. 2. Heat evolution curves: L_1, without $NaNO_3$; L_2, with 2 wt% $NaNO_3$.

deceleration period and the steady period. From Fig. 1, it can also be seen that as the hydration temperature increases, the steady period becomes less obvious. This shows that the hydration temperature has a very large effect on the hydration of $3CaO \cdot 3Al_2O_3 \cdot CaSO_4$.

3.2. *Effect of $NaNO_3$ on the hydration of $3CaO \cdot 3Al_2O_3 \cdot CaSO_4$*

Fig. 2 shows two hydration heat curves. L_1 represents the material without $NaNO_3$ and L_2 represents the material with $NaNO_3$. The properties of the hydration curves are listed in Table 2. Fig. 3 shows the integrated hydration heat for samples L_1 and L_2.

Fig. 3 shows that the integrated hydration heat is increased with the addition of the $NaNO_3$. An inspection of Fig. 2 and Table 2 shows that the starting time for the second hydration peak is reduced from 17 to 14 min in the presence of $NaNO_3$

Table 2
Hydration properties of the two samples

Sample	L_1 [a]	L_2 [b]
Peak height in mW	21	24
Peak position in min	107	98
Starting time in min	17	14
Ending time in min	150	138
Half peak width in min	128	123

[a] Without $NaNO_3$. [b] With 2 wt% $NaNO_3$.

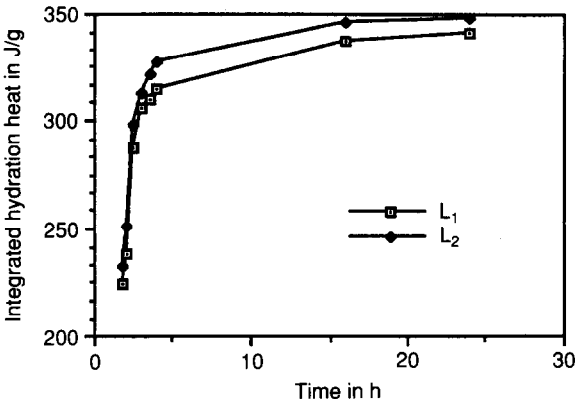

Fig. 3. Integrated hydration heat for samples L_1 and L_2.

and it is this second peak which is calculated as the integrated hydrogen heat in Fig. 3. From the results in Table 2 and Fig. 2, it can be seen that the hydration heat peak height increases from 21 to 24 mW; the time of hydration peak moves from 107 to 98 min; half peak width decreases from 128 to 123 min. These results demonstrate that adding $NaNO_3$ obviously accelerates the hydration process of $3CaO \cdot 3Al_2O_3 \cdot CaSO_4$.

3.3. *Calculation of the kinetic parameters for hydration at 45°C*

A widely used kinetic analysis equation for hydration in cement research [8] is applied in this study

$$[1-(1-\alpha)^{1/3}]^N = kt \tag{3}$$

where k is the hydration rate constant, N is the hydration order and α is the hydration extent at time t; α can be expressed as P/P_∞, where P is the hydration heat to time t and P_∞ is the total hydration heat. Sakai et al. [9] have shown that N is related to the hydration mechanism. When $N < 1$, the hydration process is in a self-catalyzed period; when $N \approx 1$, the hydration process is controlled by reaction at the edge of the crystals, and when $N > 2$, the hydration is diffusion controlled.

By taking logarithms to Eq. (3) and making plots of $\ln[1-(1-\alpha)^{1/3}]$ against $\ln t$, several linear relationship are obtained for the different hydration periods. From the linear regression results, the hydration characteristics and the mechanism for the different hydration periods can be identified.

In general, it is very difficult to obtain the total hydration heat of cements by using calorimeters. There are two methods in use at present: one is the direct method and the other the indirect method. The direct method is also called the heat flow method and measures the heat flow of the cement hydration process directly using the calorimeter. In the indirect method, the heat involved in dissolving unhydrated cement and that of hydrated cement after a certain time is noted; the difference in the two heat measurements gives the hydration heat for that period.

This method is also called the dissolving heat method. It can measure the long-term hydration heat, but the operation is very complicated and therefore the results always contain inaccuracy.

The high sensitivity and accuracy of the Calvet conducting C80 microcalorimeter were used in this study to measure the hydration products of $3CaO \cdot 3Al_2O_3 \cdot CaSO_4$ quantitatively and directly. Then, from the amount of hydration products and the corresponding hydration heat, the total hydration heat, P_∞, of $3CaO \cdot 3Al_2O_3 \cdot CaSO_4$ can be calculated.

When the reaction in Eq. (1) proceeds under 45°C for 24 h, significant amounts of ettringite, aluminum gel and unhydrated reactants are known to be formed [2]. After driving off the adsorbed moisture by heating, the sample was then subjected to a constant heating rate, 1°C min^{-1}, in the Calvet C80 microcalorimeter.

Using this temperature regime the following reactions are known to occur:

(1) The dehydration of $CaSO_4 \cdot 2H_2O$

$$CaSO_4 \cdot 2H_2O \rightarrow CaSO_4 \cdot 0.5H_2O + 1.5H_2O \quad (4)$$

$$CaSO_4 \cdot 0.5H_2O \rightarrow CaSO_4 + 0.5H_2O \quad (5)$$

(2) The dehydration of ettringite. From differential thermal analysis (DTA) data, it is known that there are two stages in the dehydration of ettringite [1]. One is the loss of 20 H_2O at temperatures between 110 and 160°C. The remainder of the water is lost around 260°C.

(3) The dehydration of aluminum gel ($Al(OH)_3$)

$$2Al(OH)_3 \rightarrow Al_2O_3 + 3H_2O$$

Fig. 4 shows the heating curves observed using the Calvet microcalorimeter. Curve B represents that of the sample. Every dehydration gives an endothermic peak, but in this complicated system, some peaks are overlapped. In order to distinguish the peaks, the dehydrations of $CaSO_4 \cdot 2H_2O$ and $Al(OH)_3$ were carried out under the same conditions and are represented as curves C and A in Fig. 4 respectively. From Fig. 4 it can be seen that: the dehydration of $CaSO_4 \cdot 2H_2O$, curve C, occurs in two stages, one represented by Eq. (4) at 121°C and the other by Eq. (5) at 166°C; the dehydration of $Al(OH)_3$, curve A, has three obvious endothermic peaks at 192, 216 and 255°C.

From the above discussion, the peaks on curve B can be explained. The first peak is caused by the dehydration of ettringite and gypsum. The second peak represents the dehydration of dehydrated gypsum ($CaSO_4 \cdot 0.5H_2O$). At this point, the dehydration of $CaSO_4 \cdot 0.5H_2O$ can be distinguished from all other components.

Let ΔH represent the enthalpy of the dehydration of $CaSO_4 \cdot H_2O$. The dehydration heat for $CaSO_4 \cdot 0.5H_2O$ in the sample can be designated as Q. Then the amount of $CaSO_4 \cdot 0.5H_2O$ in the sample is $A = Q/\Delta H$ (mol). The $CaSO_4 \cdot 0.5H_2O$ is the solid product in Eq. (4). Thus the amount of $CaSO_4 \cdot 2H_2O$ is given by $N_1 = A = Q/\Delta H$ (mol). Assuming the amount of $CaSO_4 \cdot 2H_2O$ before the hydration is N_2, then the amount of $CaSO_4 \cdot 2H_2O$ reacted is $N_c = N_2 - N_1$. It follows that the weight of ettringite in the sample is $W = N_c M_1/2 \times 166$ where

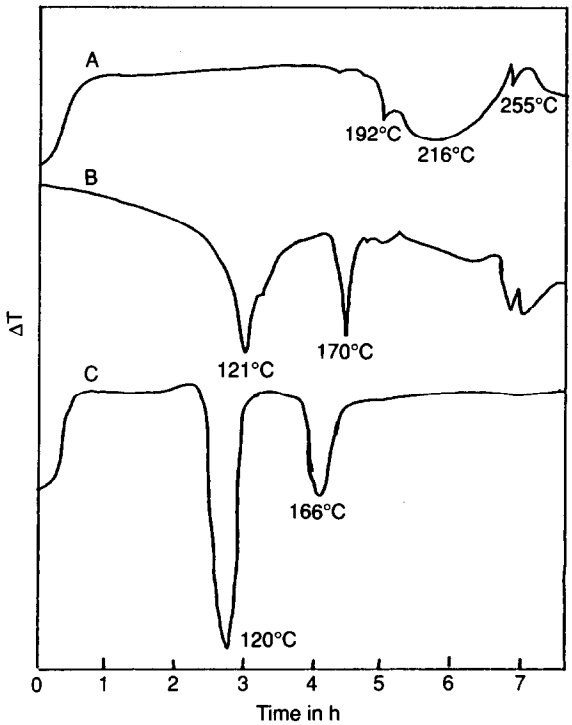

Fig. 4. Calorimeter curves: curve A, $Al(OH)_3$; curve B, the sample; and curve C, $CaSO_4 \cdot 2H_2O$.

M_1 is the formula weight of ettringite. From Eq. (1), the extent of hydration of $3CaO \cdot 3Al_2O_3 \cdot CaSO_4$ can be calculated. Using the corresponding hydration heat, P, the value of P_∞ can be obtained. Table 3 summarizes the experimental results. Table 4 gives the calculated value of P_∞ for hydration of the pure $3CaO \cdot 3Al_2O_3 \cdot CaSO_4$.

It is also found that, following a suggestion made by Knudsen [10], plotting $1/P$ vs. $1/(t - t_0)$ gives a linear relation, where t_0 is the time when the accelerating period begins. Therefore we have

$$\frac{1}{P} = C + \frac{B}{t - t_0} \tag{6}$$

Table 3
Amount of ettringite and extent of hydration [a]

Run no.	Wt. (before) in mg	Wt. (after) in mg	N_c in mol	W in mg	Hydration extent in %
1	253.4	313.4	65.97	236.9	72.17
2	233.1	288.3	61.27	219.9	72.83

[a] For meanings of symbols, see text.

Table 4
Total hydration heat of $3CaO \cdot 3Al_2O_3 \cdot CaSO_4$

Run no.	Hydration extent after 24 h in %	Heat for 24 h in J g^{-1}	P_∞ in J g^{-1} [a]	Average P_∞ in J g^{-1}
1	72.17	339.21	470.08	
2	72.83	338.54	464.84	467.46

[a] Total hydration heat.

Table 5
P_∞ and r values for samples L_1 and L_2

	P_∞ in J g^{-1}	r [a]
L_1	480.8	0.992
L_2	476.2	0.991

[a] Regression factor.

where B and C are constants. In the limit where $t = \infty$, $C = 1/P_\infty$. Thus, the intercept in the plot of $1/P$ vs. $1/(t - t_0)$ gives P_∞. Such plots for samples L_1 and L_2 were created and the results are listed in Table 5. From Table 5 it can be seen that the P_∞ values calculated from Eq. (6) are very close to those calculated by the other method (Table 4). This implies that the method based on the suggestion put forward by Knudsen is applicable and accurate. In order to compare the kinetic analysis parameters for the L_1 and L_2 samples, P_∞ values from Tables 4 and 5 are used respectively in the calculation.

Knowing P_∞, the extent of hydration, α, can be calculated. Rearrangement of Eq. (3) gives

$$\ln[1 - (1 - \alpha)^{1/3}] = a + b \ln t \tag{7}$$

where $a = (1/N) \ln k$ and $b = 1/N$. Plots of $\ln[1 - (1 - \alpha)^{1/3}]$ against $\ln t$ were made for the acceleration, deceleration and steady periods, and the linear regression parameters are listed in Tables 6 and 7. The calculated results for N and k are shown in Tables 8 and 9.

It can be seen for the hydration of pure $3CaO \cdot 3Al_2O_3 \cdot CaSO_4$ that the acceleration period is self-catalyzed with $N = 0.69$, the hydration in the deceleration

Table 6
Linear regression parameters for different hydration periods of the pure $3CaO \cdot 3Al_2O_3 \cdot CaSO_4$

Parameters	Acceleration	Deceleration	Steady
a	−3.20	−3.03	−2.69
b	1.44	1.05	0.51
r [a]	0.987	0.991	0.997

[a] Regression factor.

Table 7
a, b and r for different hydration periods of samples L_1 and L_2

Sample	Parameters	Acceleration	Deceleration	Steady
L_1	a	−3.42	−3.15	−2.76
	b	1.48	1.07	0.52
	r	0.990	0.994	0.995
L_2	a	−2.87	−2.68	−0.33
	b	1.54	1.11	0.53
	r	0.994	0.992	0.997

Table 8
k and N values of various hydration periods of $3CaO \cdot 3Al_2O_3 \cdot CaSO_4$

Parameters	Acceleration	Deceleration	Steady
k in h^{-1}	0.11	0.056	0.0051
N	0.69	0.95	1.96

Table 9
k and N values of different hydration periods for samples L_1 and L_2

Parameters	Acceleration		Deceleration		Steady	
	L_1	L_2	L_1	L_2	L_1	L_2
k in h^{-1}	0.10	0.15	0.05	0.09	0.005	0.01
N	0.68	0.65	0.93	0.90	1.92	1.89

period is controlled by the edge reaction with N close to 1, and the hydration during the steady period is diffusion-controlled with N close to 2. These results support those of Sakai et al. [9]. At the same time, the reaction rate constants decrease in the following order: the acceleration, deceleration and steady periods. This is in accordance with the hydration curve.

From Tables 5 and 9, it can be seen that when $NaNO_3$ is added: the total hydration heat of $3CaO \cdot 3Al_2O_3 \cdot CaSO_4$ decreases from 480.8 to 476.2 J g^{-1} in the acceleration period, adding $NaNO_3$ increases the hydration rate constant k from 0.10 to 0.15 h^{-1}, while N decreases from 0.68 to 0.65 which means that the hydration process is slowed down; in the deceleration period, k increases from 0.06 to 0.09 h^{-1} and N decreases from 0.93 to 0.90; in the steady period, k increases from 0.005 to 0.01 h^{-1} and N decreases from 1.92 to 1.89; in the presence of $NaNO_3$, the hydration process can still be obviously divided into three periods. The N values for the different hydration periods also support the results of Sakai et al. [9].

Table 10
k and N values of different hydration temperatures

Temp in °C		Acceleration period	Deceleration period	Steady period
30	k in h^{-1}	0.0812	0.0776	0.0154
	N	0.88	0.93	1.65
45	k in h^{-1}	0.1099	0.0562	0.0051
	N	0.69	0.95	1.96
60	k is h^{-1}	0.1687	0.0530	0.0044
	N	0.51	1.02	2.23

3.4. Effect of hydration temperature on kinetic analysis results

Following the same procedure as used for the pure $3CaO \cdot 3Al_2O_3 \cdot CaSO_4$, the kinetic analysis was performed for the hydrations at 30 and 60°C. The results are shown in Table 10.

From results in Table 10, it can be seen that the higher the hydration temperature, the higher the reaction order, N. It can be seen that when the hydration temperature increases, the reaction rate constant k values increase for the acceleration period and decrease for both the deceleration and the steady periods. This means that the hydration process is accelerated when the hydration temperature increases.

4. Conclusions

By following the hydration process of $3CaO \cdot 3Al_2O_3 \cdot CaSO_4$, the kinetic analysis shows that the use of the Calvet conducting C80 microcalorimeter can accurately and quantitatively measure the amount of the hydration product, ettringite, that was formed. The total hydration heat P_∞ and the hydration extent at time t can be calculated. This demonstrates how the Calvet microcalorimeter can be used to evaluate the kinetics of the hydration process in cement.

The hydration of $3CaO \cdot 3Al_2O_3 \cdot CaSO_4$ is divided into three periods: the acceleration period, the deceleration period and the steady period. As the hydration temperature increases, the induction period is shortened. The kinetic evaluation for hydration shows that the hydration rate constant is highest in the acceleration period. In the deceleration period, the reaction is slowed down and in the steady period, the hydration rate constant is lowest.

When small amounts of $NaNO_3$ are present, the hydration process of $3CaO \cdot 3Al_2O_3 \cdot CaSO_4$ was accelerated and each hydration period occurred earlier. From the calculations performed here, the hydration rate constant increased while the hydration order decreased. These results show that adding $NaNO_3$ shortened the time over which the hydration heat was released which is very useful for building construction during the winter.

References

[1] J.G. Xiu and Z.W. Wu, Expansive and Self-Stressing Cements and Their Engineering Application, Chinese Building Engineering Publishers, Beijing, 1985.
[2] J.A. Deng, J. Chinese Ceram. Soc., 10 (1982) 56.
[3] H.X. Yang and R.J. Tian, Conc. Cem. Prod., 2 (1986) 9.
[4] P.K. Mehta, J. Am. Ceram. Soc., 56 (1973) 315.
[5] G. Hansen, Cem. Conc. Res., 3 (1973) 658.
[6] K. Ogana and D.M. Roy, Cem. Conc. Res., 12 (1982) 101.
[7] K.G. Krasilnikow, Proc. 6th Int. Congr. Chem. Cem., Moscow, 3 (1974) 173.
[8] P. Barnes, Structure and Performances of Cements, Applied Science Publishers, London, 1983, p. 263.
[9] E. Sakai, M. Daimon and R. Kondo, Proc. 7th Congr. Chem. Cem., Paris, 2 (1980) 203.
[10] T. Knudsen, Proc. 7th Congr. Chem. Cem., Paris, 2 (1980) 170.